

Reduction of contaminants originating from primary beam by improving the beam stoppers in GARIS-II

S. Kimura^{a,*}, D. Kaji^a, Y. Ito^{b,a}, H. Miyatake^c, K. Morimoto^a, P. Schury^c, M. Wada^c

^aNishina Center for Accelerator Based Science, RIKEN, Wako, 351-0198, Japan

^bAdvanced Science Research Center, Japan Atomic Energy Agency, Tokai, Ibaraki 319-1195, Japan

^cWako Nuclear Science Center (WNSC), Institute of Particle and Nuclear Studies (IPNS), High Energy Accelerator Research Organization(KEK), Wako, 351-0198, Japan

Abstract

Two independent beam stoppers have been developed for improving the beam separation of the gas-filled recoil ion separator GARIS-II. Performance evaluation of these supplemental beam stoppers was performed by using the ^{208}Pb (^{18}O , $3n$) ^{223}Th reaction. A160-fold enhancement of the signal-to-noise ratio at the GARIS-II focal plane was observed.

Keywords: Gas-filled recoil ion separator; GARIS-II; Beam separation; Fusion-evaporation reactions

PACS: 29.30.Aj

Gas-filled recoil separators are a powerful tool for synthesis of (super)heavy elements due to their capacity to cancel out the large velocity dispersions of fusion-evaporation reaction products; they have been implemented at several facilities [1, 2, 3, 4]. At the RIKEN Nishina Center for Accelerator-Based Science, two gas-filled recoil ion separators, GARIS [5] and GARIS-II [6], have been used in the study of (super)heavy nucleosynthesis and nuclear chemistry.

In order to measure the masses of superheavy elements, an experimental campaign called SHE-mass-I, wherein GARIS-II was coupled with a multireflection time-of-flight mass spectrograph (MRTOF-MS) [7], has been initiated. Mass measurement of neutron-deficient isotopes from Bi ($Z = 83$) to Ac ($Z = 89$) [8, 9] as well as isotopes from Es ($Z = 99$) to No ($Z = 102$) [10] have already been carried out successfully.

SHE-mass-I requires the energetic beams from GARIS-II to be converted to low-energy beams before they can be analyzed with the MRTOF-MS. This is accomplished via a cryogenic gas-cell (GC) and an ion transport system that includes a multiple ion trap suite [8]. Due to space charge effects, the ion extraction efficiency of the GC would be reduced as the incoming beam rate increases [11]. A wide range of fusion evaporation reactions, with the primary beam intensity exceeding $2\text{ p}\mu\text{A}$ in some cases, have been used to produce exotic isotopes for the SHE-mass-I mass measurements. In several cases, unwanted particles with non-negligible intensities were observed to reach the GARIS-II focal plane, possibly by reducing the system efficiency and even posing a risk of damage to the GC. Thus

an enhancement in the suppression of unwanted particles was required. We report here on the development of such an improved suppression system.

The primary beam and the evaporation residues differ in terms of their behavior in GARIS-II based on their $B\rho$ -values and angular distributions immediately after the target. Their $B\rho$ -values are generally similar to each other, as discussed above, although there remains a capability to separate them by the small differences of their trajectories at the exit of the first dipole (D1) of GARIS-II. Evaporation residues have large angular distributions compared to the primary beam, due mainly to multiple scattering in the target materials and recoils of evaporated light-particles in de-excitation processes. As such, primary beam and

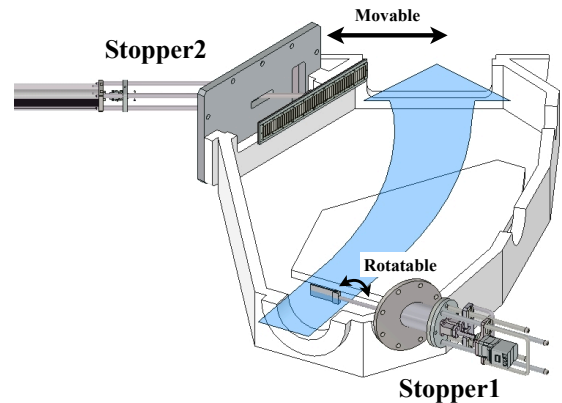


Figure 1: Schematic view of the primary beam stoppers. The D1 chamber is shown in cross-section. The blue arrow indicates the beam direction. This figure presents an operational state where Stopper1 has an effective area of 24 cm^2 while Stopper2 is at the 0 cm position.

*Corresponding author

Email address: sota.kimura@riken.jp (S. Kimura)

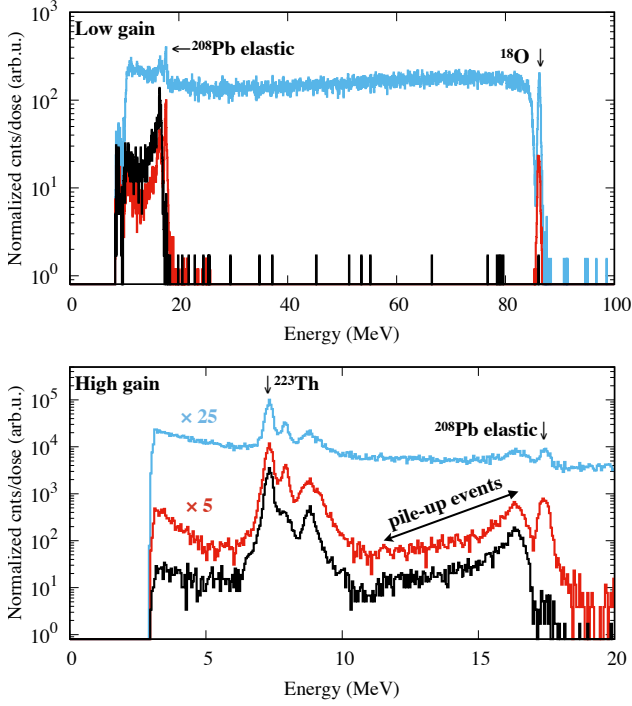


Figure 2: Energy spectra of the silicon detector array. (Blue line) Energy spectrum without either stoppers or primary beam chopping. (Black line) Energy spectrum with primary beam chopping. (Red line) Energy spectrum with both stoppers and without primary beam chopping.

evaporation residues could be separated by utilizing the differences in their angular distributions.

For separating the primary beams and the evaporation residues, two water-cooled primary beam stoppers, “Stopper1” and “Stopper2”, were designed and installed in the D1 chamber of GARIS-II as shown in Fig. 1. Stopper1, installed at the entrance of the D1 chamber, consisted of a copper plate of 8 cm width and 3 cm height. It was possible to vary the effective area it presented to the beam by rotating the structure. Stopper2, located near the D1 chamber exit, was made of a 40 cm wide and 6 cm high copper board mounted on a linear manipulator to change its position; tantalum fins on its surface prevented scattering of impinging particles.

The performance of the stoppers were evaluated by using the ^{208}Pb (^{18}O , $3n$) ^{223}Th reaction. A 4.84 MeV/u $^{18}\text{O}^{5+}$ beam with average intensity of 16 pA was provided by the RIKEN linear accelerator RILAC. The ^{208}Pb target segments were prepared by evaporation onto 60 $\mu\text{g}/\text{cm}^2$ carbon backings until an average thickness of 450 $\mu\text{g}/\text{cm}^2$ was achieved. The target segments were mounted on a 30 cm diameter target wheel [12] that was nominally rotated at 2000 rpm during irradiation.

An array of silicon detectors (HAMAMATSU S3204-09), arranged in a 3×5 pattern, was employed to count both the incoming ^{223}Th and contaminants reaching the GARIS-II focal plane. Signals of the detector array were

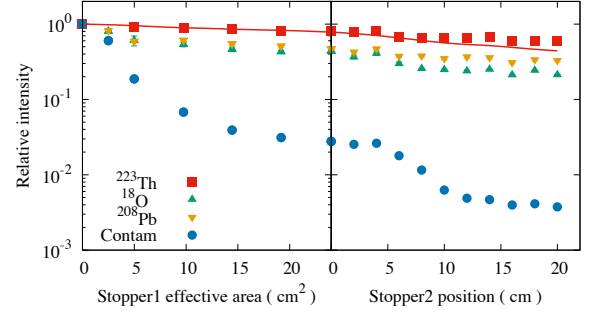


Figure 3: Results of both stoppers' performance evaluations. The figures indicate the dependencies of the counting rates on the Stopper1 effective area (left) and on the Stopper2 position (right). Size of the all error bars are smaller than the points. Red line represents the result of ^{223}Th transport simulations.

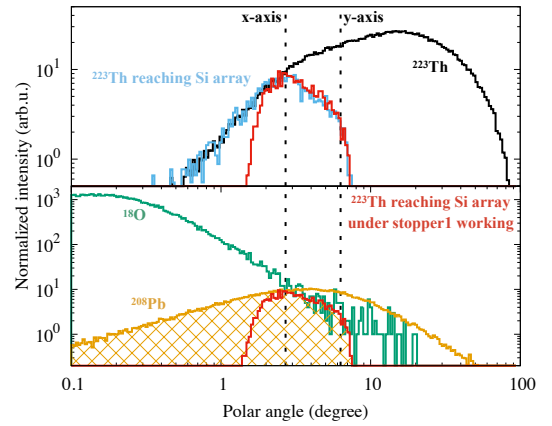


Figure 4: Simulated polar angle distribution right after the target. (Black line) Simulated result of ^{223}Th without gate. (Blue line) ^{223}Th result gated with a condition that reaching the silicon detector array installed at the GARIS-II focal plane. (Red lines) Same gate as the blue line, but simulated result under the assumption that stopper1 fully works. (Green line) Simulated result of ^{18}O . (Orange line) Result of ^{208}Pb assuming zero-degree recoil. (Dotted lines) GARIS-II acceptance of x- and y-axis. See the text for the details of simulations.

processed with both high- and low-gain circuits. The primary beam was chopped to measure the α -decay from ^{223}Th under low-background conditions. The beam chopping sequence was chosen to be 0.2 sec beam on and 0.2 sec beam off. Energy spectra as measured by both high- and low-gain circuits are shown in Fig. 2. The high-gained data were used for counting the ^{223}Th events, where the intensities were determined by Gaussian fitting. The intensities of the contaminants were obtained from integration of the low-gain data down to 17 MeV, which is a border between the ^{208}Pb elastic events and the pile-up events of fast decay of ^{223}Th 's granddaughter ^{215}Rn ($t_{1/2} = 2.3 \mu\text{s}$). Because of this ambiguity, low energy contaminant events are not included in the present analysis. Counts of ^{18}O and ^{208}Pb events were determined via Gaussian fitting of the low- and high-gained data, respectively.

The evaluation results are shown in Fig. 3. In the present case, the 4+ state of the ^{18}O beam after the tar-

gets has a $B\rho$ -value that is close to the optimum for ^{223}Th : $B\rho(^{18}\text{O})/B\rho(^{223}\text{Th}) = 0.985$. An intensity ratio of the rate of contaminants to the rate of ^{223}Th of ~ 20 was determined without either stopper. As the Stopper1 effective area began to increase, the intensity of the contaminants rapidly decreased; in contrast, the ^{223}Th counting rate varied only gradually (left panel of Fig. 3). As a result, we could suppress $\sim 97\%$ of the contaminants from reaching the focal plane by using Stopper1, while $\sim 80\%$ of ^{223}Th was still transported. The same measurements were conducted by changing the Stopper2 position as shown in the right panel of Fig. 3. When measuring the Stopper2 performance, the Stopper1 effective area was set to its maximum value of 24 cm^2 . The Stopper2 measurement shows results similar to those obtained with Stopper1. Thus, in the end, we can improve the signal-to-noise ratio by a factor of ~ 160 by using both stoppers.

Red line shown in Fig. 3 indicates the simulated result of ^{223}Th transport in GARIS-II based on Geant4 [13], including consideration of recoil of evaporated particle in the de-excitation process, charge exchange processes between the GARIS-II buffer gas and ions, scattering by materials including the buffer gas, and the GARIS-II geometry including both stoppers and optics. The simulation reproduces the trend of reduction of ^{223}Th transmission efficiency by the use of Stopper1. Figure 4 shows the simulated polar angular distribution right after the target. This indicates that ^{223}Th events only having limited polar angle can reach the GARIS-II focal plane. The reduction rate of ^{208}Pb elastic events by Stopper1 can be explained via Fig. 4. Assuming that the ^{208}Pb events reaching the GARIS-II focal plane have the same angular distribution as the ^{223}Th events reaching the GARIS-II focal plane, the reduction rate can be represented by a ratio of the area surrounded by the red line to the orange-colored mesh area and is found to be 45%. This value is consistent with the experimental value of 47.3(2.4)%. But, in contrast with this, the reduction rate of ^{18}O cannot be explained in the same way. The reason for this is incompletely understood and further investigation is necessary. Because the reaction used in the present study is very asymmetric and the evaporation residues have wide initial angular distributions, the peak lies the outside of the acceptable region. This implies that the beam stoppers could even better improve the signal-to-noise ratio for more symmetric reactions.

The contaminant events can be sorted into two categories: peaks and continuous. As indicated in Fig 2, both stoppers mainly reduce the continuous components. For the production mechanisms of the continuous components having wide energy range, some mechanisms such as deep inelastic reaction, scattering with beam line inner walls, etc., can be considered. But it is difficult to identify the origin of the continuous components based the information of energy spectra only. Thus further investigations are necessary to understand the origin of the contaminants and achieve a maximally low-background environment at the

GARIS-II focal plane.

In order to improve the signal-to-noise ratio at the GARIS-II focal plane, two independent beam stoppers have been developed. Performance evaluations of the beam stoppers were performed by using the $^{208}\text{Pb}(^{18}\text{O}, 3n)^{223}\text{Th}$ reaction. This study indicates a 160-fold enhancement of the signal-to-noise ratio at the GARIS-II focal plane has been achieved by using the beam stoppers. We demonstrate that a simple mechanism can drastically reduce the contaminants at the GARIS-II focal plane while maintaining the intensity of the desired fusion-evaporation reaction products. An initial application of the beam stoppers is reported in [14].

We would like to express our sincere gratitude to the RIKEN Nishina Center for Accelerator-Based Science and the Center for Nuclear Science at the University of Tokyo for their support of the present measurements. This study was supported by the Japan Society for the Promotion of Science KAKENHI, Grant Number 24224008, 15H02096, 15K05116, and 17H06090.

References

- [1] K. Subotic, Y. Oganessian, V. Utyonkov, Y. Lobanov, F. Abdullin, A. Polyakov, Y. Tsyganov, O. Ivanov, Evaporation residue collection efficiencies and position spectra of the dubna gas-filled recoil separator, Nuclear Instruments and Methods in Physics Research Section A: Accelerators, Spectrometers, Detectors and Associated Equipment 481 (1) (2002) 71 – 80. doi:[http://dx.doi.org/10.1016/S0168-9002\(01\)01367-5](http://dx.doi.org/10.1016/S0168-9002(01)01367-5). URL <http://www.sciencedirect.com/science/article/pii/S0168900201013675>
- [2] K. Gregorich, Simulation of recoil trajectories in gas-filled magnetic separators, Nuclear Instruments and Methods in Physics Research Section A: Accelerators, Spectrometers, Detectors and Associated Equipment 711 (2013) 47 – 59. doi:<https://doi.org/10.1016/j.nima.2013.01.020>. URL <http://www.sciencedirect.com/science/article/pii/S0168900213000673>
- [3] J. M. Gates, C. E. Düllmann, M. Schädel, A. Yakushev, A. Türler, K. Eberhardt, J. V. Kratz, D. Ackermann, L.-L. Andersson, M. Block, W. Bröchle, J. Dvorak, H. G. Essel, P. A. Ellison, J. Even, U. Forsberg, J. Gellanki, A. Gorshkov, R. Graeger, K. E. Gregorich, W. Hartmann, R.-D. Herzberg, F. P. Heßberger, D. Hild, A. Hübner, E. Jäger, J. Khuyagbaatar, B. Kindler, J. Krier, N. Kurz, S. Lahiri, D. Liebe, B. Lommel, M. Maiti, H. Nitsche, J. P. Omtvedt, E. Parr, D. Rudolph, J. Runke, H. Schaffner, B. Schausten, E. Schimpf, A. Semchenkov, J. Steiner, P. Thörle-Pospiech, J. Uusitalo, M. Wegrzecki, N. Wiehl, First superheavy element experiments at the gsi recoil separator tasca: The production and decay of element 114 in the $^{244}\text{Pu}(^{48}\text{Ca}, 3-4n)$ reaction, Phys. Rev. C 83 (2011) 054618. doi:[10.1103/PhysRevC.83.054618](https://doi.org/10.1103/PhysRevC.83.054618). URL <https://link.aps.org/doi/10.1103/PhysRevC.83.054618>
- [4] M. Leino, J. Äystö, T. Enqvist, P. Heikkinen, A. Jokinen, M. Nurmi, A. Ostrowski, W. Trzaska, J. Uusitalo, K. Eskola, P. Armbruster, V. Ninov, Gas-filled recoil separator for studies of heavy elements, Nuclear Instruments and Methods in Physics Research Section B: Beam Interactions with Materials and Atoms 99 (1) (1995) 653 – 656, application of Accelerators in Research and Industry '94. doi:[https://doi.org/10.1016/0168-583X\(94\)00573-7](https://doi.org/10.1016/0168-583X(94)00573-7). URL <http://www.sciencedirect.com/science/article/pii/0168583X94005737>

- [5] K. Morita, A. Yoshida, T. Inamura, M. Koizumi, T. Nomura, M. Fujioka, T. Shinozuka, H. Miyatake, K. Sueki, H. Kudo, Y. Nagai, T. Toriyama, K. Yoshimura, Y. Hatsukawa, Riken isotope separator on-line garis/igisol, Nuclear Instruments and Methods in Physics Research Section B: Beam Interactions with Materials and Atoms 70 (1) (1992) 220 – 225. doi:[https://doi.org/10.1016/0168-583X\(92\)95935-K](https://doi.org/10.1016/0168-583X(92)95935-K). URL <http://www.sciencedirect.com/science/article/pii/S0168583X9295935K>
- [6] D. Kaji, K. Morimoto, N. Sato, A. Yoneda, K. Morita, Gas-filled recoil ion separator garis-ii, Nuclear Instruments and Methods in Physics Research Section B: Beam Interactions with Materials and Atoms 317, Part B (2013) 311 – 314. doi:<http://dx.doi.org/10.1016/j.nimb.2013.05.085>. URL <http://www.sciencedirect.com/science/article/pii/S0168583X13007039>
- [7] P. Schury, M. Wada, Y. Ito, F. Arai, S. Naimi, T. Sonoda, H. Wollnik, V. Shchepunov, C. Smorra, C. Yuan, A high-resolution multi-reflection time-of-flight mass spectrograph for precision mass measurements at RIKEN/SLOWRI, Nuclear Instruments and Methods in Physics Research Section B: Beam Interactions with Materials and Atoms 335 (2014) 39 – 53. doi:<http://dx.doi.org/10.1016/j.nimb.2014.05.016>. URL <http://www.sciencedirect.com/science/article/pii/S0168583X1400559X>
- [8] P. Schury, M. Wada, Y. Ito, D. Kaji, F. Arai, M. MacCormick, I. Murray, H. Haba, S. Jeong, S. Kimura, H. Koura, H. Miyatake, K. Morimoto, K. Morita, A. Ozawa, M. Rosenbusch, M. Reponen, P.-A. Söderström, A. Takamine, T. Tanaka, H. Wollnik, First online multireflection time-of-flight mass measurements of isobar chains produced by fusion-evaporation reactions: Toward identification of superheavy elements via mass spectroscopy, Phys. Rev. C 95 (2017) 011305. doi:[10.1103/PhysRevC.95.011305](https://doi.org/10.1103/PhysRevC.95.011305). URL <http://link.aps.org/doi/10.1103/PhysRevC.95.011305>
- [9] M. Rosenbusch, Y. Ito, P. Schury, M. Wada, D. Kaji, K. Morimoto, H. Haba, S. Kimura, H. Koura, M. MacCormick, H. Miyatake, J. Y. Moon, K. Morita, I. Murray, T. Niwase, A. Ozawa, M. Reponen, A. Takamine, T. Tanaka, H. Wollnik, New mass anchor points for neutron-deficient heavy nuclei from direct mass measurements of radium and actinium isotopes, Phys. Rev. C 97 (2018) 064306. doi:[10.1103/PhysRevC.97.064306](https://doi.org/10.1103/PhysRevC.97.064306). URL <https://link.aps.org/doi/10.1103/PhysRevC.97.064306>
- [10] Y. Ito, P. Schury, M. Wada, F. Arai, H. Haba, Y. Hirayama, S. Ishizawa, D. Kaji, S. Kimura, H. Koura, M. MacCormick, H. Miyatake, J. Y. Moon, K. Morimoto, K. Morita, M. Mukai, I. Murray, T. Niwase, K. Okada, A. Ozawa, M. Rosenbusch, A. Takamine, T. Tanaka, Y. X. Watanabe, H. Wollnik, S. Yamaki, First direct mass measurements of nuclides around $z = 100$ with a multireflection time-of-flight mass spectrograph, Phys. Rev. Lett. 120 (2018) 152501. doi:[10.1103/PhysRevLett.120.152501](https://doi.org/10.1103/PhysRevLett.120.152501). URL <https://link.aps.org/doi/10.1103/PhysRevLett.120.152501>
- [11] A. Takamine, M. Wada, Y. Ishida, T. Nakamura, K. Okada, Y. Yamazaki, T. Kambara, Y. Kanai, T. M. Kojima, Y. Nakai, N. Oshima, A. Yoshida, T. Kubo, S. Ohtani, K. Noda, I. Katayama, P. Hostain, V. Varentsov, H. Wollnik, Space-charge effects in the catcher gas cell of a rf ion guide, Review of Scientific Instruments 76 (10) (2005) 103503. doi:<http://dx.doi.org/10.1063/1.2090290>. URL <http://scitation.aip.org/content/aip/journal/rsi/76/10/10.1063/1.2090290>
- [12] D. Kaji, K. Morimoto, Double-layered target and identification method of individual target correlated with evaporation residues, Nuclear Instruments and Methods in Physics Research Section A: Accelerators, Spectrometers, Detectors and Associated Equipment 792 (2015) 11 – 14. doi:<http://doi.org/10.1016/j.nima.2015.04.042>. URL <http://www.sciencedirect.com/science/article/pii/S0168900215005306>
- [13] S. Agostinelli, et al., Geant4a simulation toolkit, Nuclear Instruments and Methods in Physics Research Section A: Accelerators, Spectrometers, Detectors and Associated Equipment 506 (3) (2003) 250 – 303. doi:[https://doi.org/10.1016/S0168-9002\(03\)01368-8](https://doi.org/10.1016/S0168-9002(03)01368-8). URL <http://www.sciencedirect.com/science/article/pii/S0168900203013688>
- [14] S. Kimura, Y. Ito, D. Kaji, P. Schury, M. Wada, H. Haba, T. Hashimoto, Y. Hirayama, M. MacCormick, H. Miyatake, J. Moon, K. Morimoto, M. Mukai, I. Murray, A. Ozawa, M. Rosenbusch, H. Schatz, A. Takamine, T. Tanaka, Y. Watanabe, H. Wollnik, Atomic masses of intermediate-mass neutron-deficient nuclei with relative uncertainty down to 35-ppb via multireflection time-of-flight mass spectrograph, International Journal of Mass Spectrometry 430 (2018) 134 – 142. doi:<https://doi.org/10.1016/j.ijms.2018.05.001>. URL <http://www.sciencedirect.com/science/article/pii/S1387380617304220>